Photoelectron spectroscopy study of GeSn epitaxial layers for photonic applications

M Bouschet, Eugénie Martinez, J M Fabbri, L Casiez, A Quintero, J da Fonseca, C Jany, P Rodriguez, A Chelnokov, J M Hartmann, et al.

Photoelectron spectroscopy study of GeSn epitaxial layers for photonic applications

M. Bouschet[1], E. Martinez[1], J. M. Fabbri[1], L. Casiez[1], A. Quintero[1], J. Da Fonseca[1], C. Jany[1], P. Rodriguez[1], A. Chelnokov[1], J.M. Hartmann[1], V. Reboud[1] and O. Renault[1]

[1]*Univ. Grenoble Alpes, CEA, Leti, 17 rue des Martyrs, F-38000Grenoble, France*

Abstract: We have investigated with X-ray Photoelectron Spectroscopy (XPS) the impact of different wet cleanings on the surface of thick GeSn 13% direct band-gap layers grown on germanium strain relaxed buffers. The XPS time-dependent study showed a fast Ge re-oxidation after only a few minutes, while tin was more stable. A dip in $(NH_4)_2S$ after the 5 min surface treatment with HCl/HF (1% / 10%) slowed germanium re-oxidation. Optimized surface cleanings enabled us to investigate GeSn band structure by momentum-resolved Photo-Emission Electron Microscopy (*k*PEEM). The obtained band structure images of an ex-situ prepared GeSn 13% surface were discussed.

1. Introduction

GeSn-based layers with high Sn contents have recently garnered huge interest, with demonstrations of lasing effects under optical [1, 2, 3, 4, 5] and electrical [6] pumping. The control of the Sn content and strain in thick GeSn alloys indeed offers possibilities of having direct band-gap semiconductors and of tuning their lasing wavelengths [7]. In addition, GeSn is a promising candidate for use in next-generation Metal Oxide Semiconductor Field Effect Transistors (MOSFETs) [8]. Indeed, hole mobility is boosted in compressively-strained GeSn channels grown on Ge Strain-Relaxed-Buffers (SRBs), electron mobility should be improved in tensile-strained Ge channels on top of GeSn SRBs and so on [9,10]. GeSn was for instance used in compressive stressors to boost the hole mobility in Ge p-type MOSFETs [11, 12] and its direct band gap properties called upon to fabricate low power Tunnel-FETs [13, 14].

The surface preparation of those metastable alloys is being investigated to (i) efficiently contact GeSn layers, (ii) deposit high-k dielectrics on GeSn with a reduced interface state density for MOSFETs and (iii) passivate surfaces to improve optoelectronic devices performances. Having an efficient surface cleaning of GeSn alloys would also enable the precise characterization of their electronic properties by angle-resolved photoelectron spectroscopy (ARPES) with state-of-the-art laboratory instruments. To date, only a few works have been published on the surface preparation of GeSn layers. A HF/HCl wet cleaning was used on $Ge_{0.94}Sn_{0.06}$ layers prior to high-k dielectrics deposition [15, 16, 17, 18]. Dips in $(NH_4)_2S$ prior to high-k dielectrics deposition were used to fabricate $Ge_{0.958}Sn_{0.042}$ channel p-MOSFETs [19]. A dip in diluted HF for 1 min followed by a $(NH_4)_2S$ dip for 30 min was used to remove GeSn native oxides prior to $Ge_{0.9}Sn_{0.1}$ p-MOS capacitors fabrication [20]. The high air reactivity of GeSn alloys was monitored by ex-situ XPS [21] and in-situ XPS [22] using combinations of diluted HF and argon plasma on $Ge_{0.85}$ $Sn_{0.15}$ layers to efficiently remove surface oxides with a reduced impact on surface roughness. Those surface preparations were used to obtain efficient nickel stanogermanides on GeSn layers [23, 24, 25]. M. A. Mahjoub *et al.* evaluated the efficiency of dips in HF, HCl and HF/HCl to remove Ge and Sn native oxides on $Ge_{0.9}Sn_{0.1}$ surfaces [26]. All the above-mentioned studies were conducted on thin, fully compressively strained GeSn layers grown on Ge SRBs.

By contrast, we investigate here the impact of wet treatments on thick, quasi-relaxed, and direct band-gap GeSn 13% layers. Thick GeSn layers contrary to pseudomorphic ones allow the effective light propagation into the active region to be used for lasers [1-6, 27], photodetection [28] or modulation [29]. Our aim is to remove surface oxide and adventitious carbon for future processes such as metallization or high-k dielectrics deposition and surface analysis by ARPES. A precise knowledge of the band structure of GeSn alloys is indeed key to better understand the physical properties of the material and its influence on device performances. We will focus here on the GeSn wet cleaning and surface preparation before photoemission electron microscopy (PEEM) measurements, to avoid fast native reoxidation of GeSn surfaces before ARPES measurements in a momentum-resolved photoemission electron microscope (*k*PEEM). We implement tentative *k*PEEM measurements on *ex situ*-grown GeSn alloys, ultimately aiming at reliably measuring their band structure and at improving our understanding of their surface electronics. Ultimately, we wish to link them to the performances of photonic devices, especially regarding the issue of inter sub-bands absorption and relationship between hole mobility and surface stress state.

2. Experimental details

480 nm thick GeSn layers were grown at 325°C on Germanium strain relaxed buffers (SRBs) in a 200 mm Epi Centura 5200 RPCVD tool using Ge_2H_6 and $SnCl_4$ precursors (Figure 1a). Homogenous GeSn layers with a Sn content of 13% were obtained on the whole surface of 200 mm wafers (Figure 1b). Cross-sectional Transmission Electron Microscopy (TEM) investigation showed the high crystalline quality of those 480 nm thick GeSn 13% layers away from the Ge SRB/GeSn interface. Dislocation arrays can be seen at the Ge-GeSn interface and only a few dislocations are observed at the TEM scale in the Ge and GeSn bulk (Figure 1c). Growth details and GeSn crystalline quality can be found in Refs. [30,31].

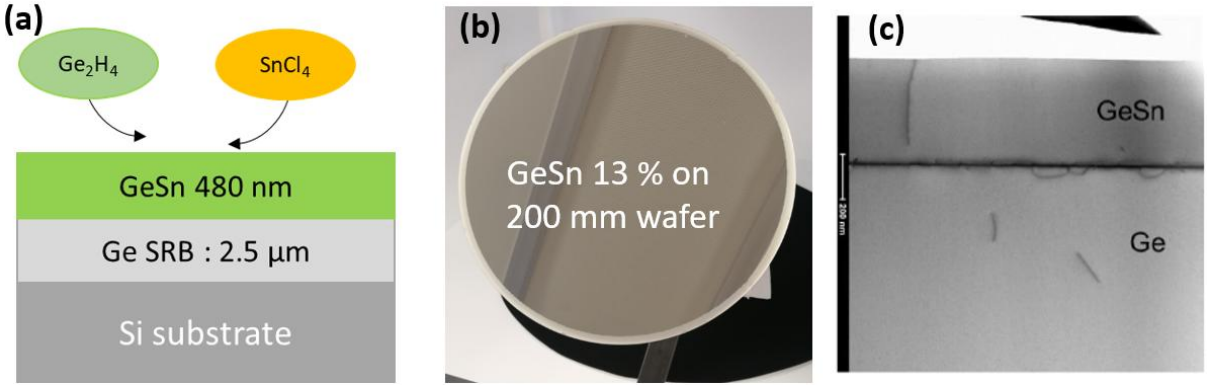

Figure 1: (a) Schematic of GeSn growth at 325°C, 100 Torr, (b) Picture of a 200mm wafer with a 480 nm thick GeSn 13% layer on top of a Ge SRB, (c) cross-sectional TEM image of that 480 nm thick GeSn 13% layer.

Samples' surfaces were treated with seven different strategies and compared to unprocessed samples (H1) (table 1): dips for 1 or 5 minutes in diluted HCl/HF 1%-1% or HCl/HF 5%-1%(H2 to H5), dips for 5 minutes in diluted HF with a 1% molar concentration in water (H6), dips in HCl/HF 10%-1% for 1 minute (H7) and, finally dips in HCl/HF 37%-1% for 5 minutes (H8). A diluted HCl/HF 5%-1% solution means that mother solutions of HCl and HF are diluted with deionized water to obtain a volumetric fraction of 5% HCl and 1% HF into a final solution of 100 mL. All surface treatments were performed at 22°C and all samples were dried under N_2 after each treatment. The surface roughness before and after wet treatments was quantified with atomic force microscopy (AFM) measurements in a Bruker AFM Dimension ICON.

The surface composition of the GeSn surface was first investigated by X-ray photoelectron spectroscopy (XPS) to estimate the relative amounts of germanium oxide and tin oxide. XPS measurements were performed under ultrahigh vacuum with an X-ray microprobe (beam size 100

μm) photoelectron spectrometer (PHI 5000 VersaProbe-II) fitted with a monochromatic Al Kα source (hν = 1486.6 eV). The overall energy resolution (spectrometer broadening and X-ray bandwidth) was 0.6 eV. The binding energy scale was set to the $4f_{7/2}$ transition of clean gold (83.96 eV) and the 2p transition of clean copper (932.62 eV). The Ge $2p_{3/2}$ and Sn $3d_{5/2}$ XPS peaks were recorded to study the oxidation of GeSn surfaces after the wet treatments listed in Table 1. Measurements were carried out at a take-off angle of 45°, yielding sampling depths of 2 and 5 nm, respectively from Ge $2p_{3/2}$ and Sn $3d_{5/2}$ photoelectrons.

Acronym	Chemical solution	Treatment time
H1	As grown	-
H2	HCl/HF 1%-1%	1 min
H3	HCl/HF 1%-1%	5 min
H4	HCl/HF 5%-1%	1 min
H5	HCl/HF 5%-1%	5 min
H6	HF 1%	5 min
H7	HCl/HF 10%-1%	5 min
H8	HCl/HF 37%-1%	5 min

Table 1: Summary of wet treatments used to clean 480 nm thick GeSn 13% layers.

Finally, ARPES measurements were performed at the micron-scale in ultra-high vacuum conditions and at ambient temperature using a NanoESCA MkI spectromicroscope (ScientaOmicron), consisting of a photoemission electron microscope (PEEM) and an aberration-compensated imaging spectrometer [32,33]. The instrument is a separate UHV chamber from the XPS, thereby necessitating sample transfer between the two systems, after the XPS measurements. This was performed under inert N_2 overpressure in a transfer vessel which was can be adapted on a special load-lock chamber of the PEEM set-up. An He I cold cathode lamp (*hv*=21.2 eV) was used as a laboratory, vacuum-ultra-violet (VUV) excitation source impinging the sample in an *off*-normal direction (65° with respect to the sample normal). So-called *k*PEEM, momentum-resolved images were acquired from a typical area of 20 μm on the surface, over the full 1st Brillouin zone (±1.8 Å^{-1}) and an energy range of 5 eV below the Fermi level. The high energy resolution momentum images were recorded at a spectrometer pass energy of 50 eV and a 1 mm diameter entrance slit of the imaging spectrometer (equivalent to an overall energy resolution of ~ 0.2 eV). The *k*-space scale was calibrated by measuring the known reciprocal lattice distances of a freshly prepared Cu (111)

single crystal surface with the same PEEM settings as for the GeSn samples. After the flat-field and dark-noise subtraction correcting for detector imperfections, the second derivative of each image series was used to enhance the contrast of the bands dispersion.

3. Results and discussion

3.1 GeSn surface preparation

As only a few nm of material are probed, band structure measurements require high crystalline quality surfaces free from oxides. In Section 2, we described the eight wet treatments (table 1) based on HF and HCl we used to remove the GeSn native oxide and clean the surface. The chemical nature of $Ge_{0.87}Sn_{0.13}$ surfaces before and after wet treatments was first evaluated using XPS. The strong reduction of GeO_x/GeO_2 and SnO_x/SnO_2 contributions can be observed on the Ge $2p_{3/2}$ and Sn $3d_{5/2}$ spectra in Figure 2a and Figure 2b, with a significant decrease of the surface oxides for H2 to H6 treatments with respect to the uncleaned sample (H1). The inset of Figure 2 shows, as a function of the treatment applied, the fraction of oxidized germanium in both GeO and GeO_2 states (a) and oxidized tin in the same states (b), both with respect to the overall germanium or tin content. These figures are obtained by peak fitting of the XPS core-level spectra using Multipack^{TM} software, and providing access to the various chemical-state components of the spectrum, as seen in more details further below (Figure 5).

We can observe that the GeO_x contribution area was not impacted by the dipping time (1, 5, or 10 minutes) and the addition or not of various amounts of HCl to the mixture. On the contrary, the SnO_x contribution area was more influenced by the dipping time and the addition or not of HCl (inset of Figure 2b). The most efficient deoxidation for strategies H2 to H6 was achieved with the H5 recipe(5 minutes dip in a HCl/HF 5%-1% solution). The H7 treatment with a larger HCl concentration yielded even lower GeOx and SnOx contributions than strategies H2 to H6.

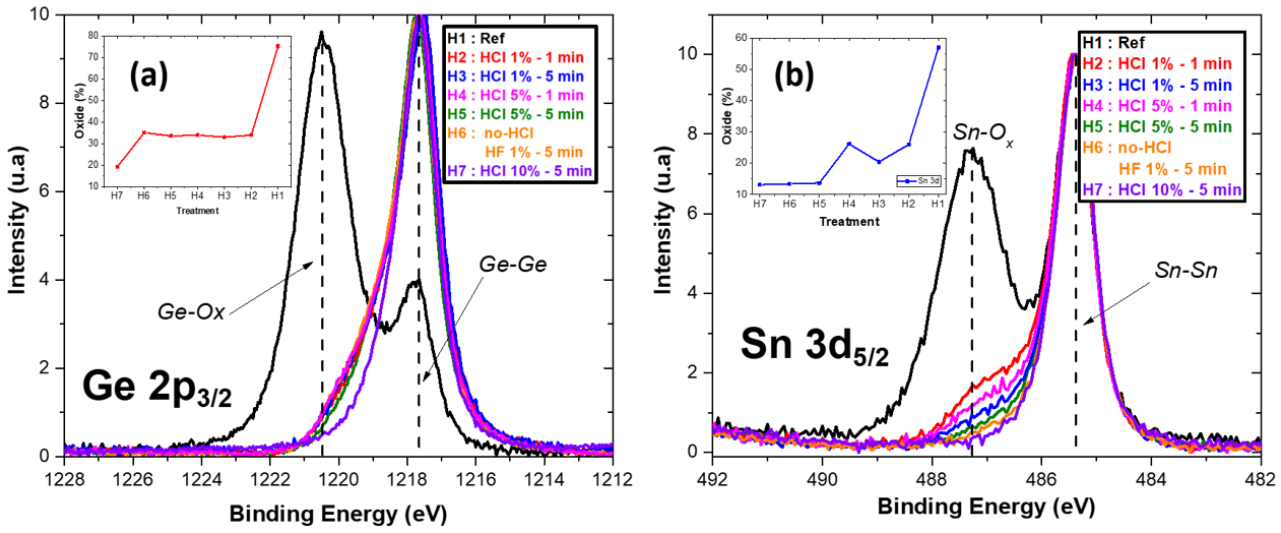

Figure 2: (a) $Ge2p_{3/2}$ XPS spectra before and after 1 minute or 5 minutes dips in various types of HF/HCl mixtures (see Table I). Inset: GeOx relative concentration after the various surface treatments listed in the figure, (b) $Sn3d_{5/2}$ XPS spectra before and after dips in various types of HF/HCl mixtures. Inset: SnOx contribution area extracted from XPS after the various surface treatments listed in the figure.

AFM images of an as-grown GeSn 13% surface and the same layer after a H7 treatment can be found in Figures 3a and 3b, respectively. Surface root means square roughnesses were found similar: 1.37 nm for the as-grown layer and 1.28 nm after the H7 treatment. The surface was cross-hatched in both cases. It was due to plastic strain relaxation in the Ge SRB underneath, with the threading arms of misfit dislocations propagating on (111) planes and leaving in their wake <110> surface undulations [7, 30, 31].

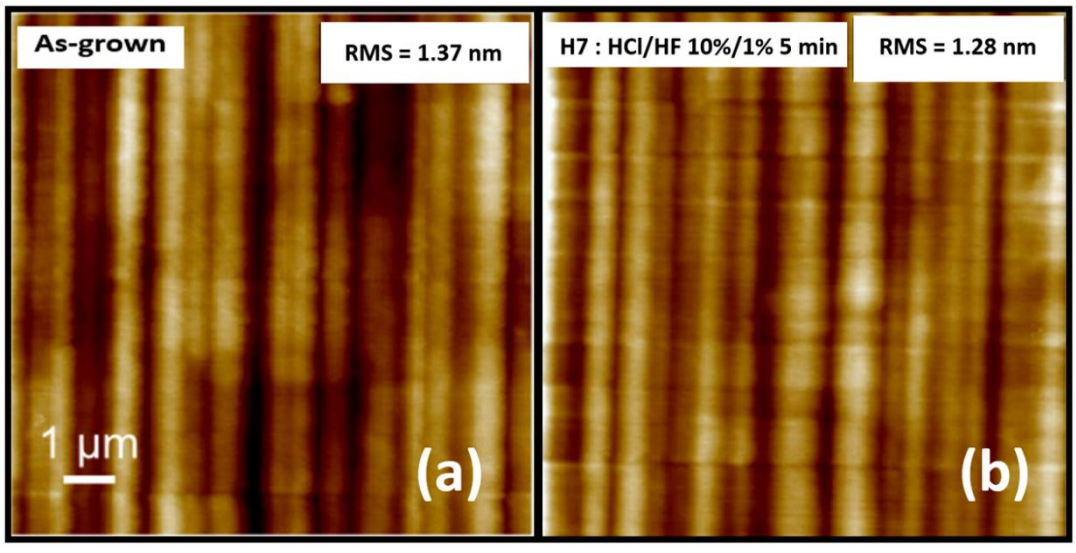

Figure 3: 10×10 µm² AFM images of (a) reference as-grown 480 nm thick GeSn 13% sample and (b) a GeSn surface after a dip for 5 minutes in HCl/HF 10%-1% (H7).

We then investigated by XPS the removal of carbon from the surface. The C 1s peak at around 285 eV was recorded for three following surface treatments: H6, H7, and H8. These measurements showed that the HCl solution was the most efficient to reduce the amount of carbon and the H6 the less efficient one. The H7 solution yielded the best trade-off between carbon removal and efficient surface de-oxidation (Figures 2a, 2b, and 4a) while preserving a good surface quality in terms of minimal roughness.

In order to investigate the stability of the 13% GeSn surface after an H7 surface cleaning, we studied the GeSn surface re-oxidation upon extended exposure to the ambient air. A fast native oxide regrowth was observed after 5, 10, 20, and 30 min (Figure 4b). It typically took us 3 minutes to dry then load GeSn samples in the XPS spectrometer, and then, less than 15 minutes for the transfer in UHV (pressure in the 10^{-8} mbar range). The inset of Figure 4b shows the growth of tin oxide and germanium oxide versus time. A preferential regrowth of germanium oxide is observed (nearly 45 % of the Ge $2p_{3/2}$ total area for the longest air exposure) compared to the tin oxide (almost 20% of the Sn 3d total area).

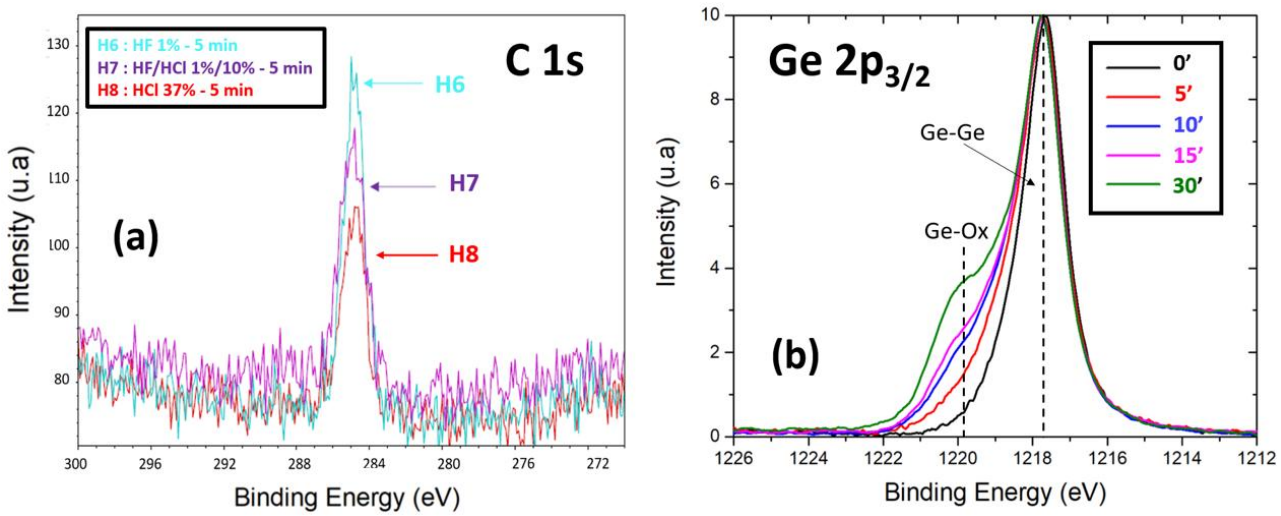

Figure 4: (a) C 1s spectra of $Ge_{0.87}Sn_{0.13}$ surfaces after a 5 min. dip in HF 1% (H6, blue curve), a 5 min dip in HCl/HF 10%-1% (H7, violet curve), and a 5 min dip in HCl 37% (H8, red curve). (b) $Ge2p_{3/2}$ XPS spectra showing the GeOx re-growth after lengthy exposures to the air of GeSn surfaces that were regenerated thanks to 5 min dips in HCl/HF 10%-1% (H7).

Several works showed the usefulness of Ge-S bonds to passivate Ge-based surfaces [26, 34]. We thus investigated the use of $(NH_4)_2S$ to protect thick, quasi-relaxed GeSn surfaces. Three protocols were used (summarized in Table 2). The P1 protocol consisted of dipping GeSn samples for 5 min in HCl/HF 10%-1% (e.g. the H7 surface preparation) followed by a second dip in an $(NH_4)_2S$ solution and a De-Ionized Water (DIW) rinsing. The P2 protocol was similar to P1, with the addition of another DIW rinse between the H7 surface preparation and the dip in $(NH_4)_2S$.

Finally, the P3 protocol consisted of a single dip in $(NH_4)_2S$ followed by a DIW rinse. No HF/HCl treatment was indeed used in protocol P3. All surface treatments were performed at 22°C and samples were dried under N_2 after each treatment.

All treated GeSn samples were placed under ultra-high vacuum (10^{-9} mbar) after a 40 min air exposure. Figure 5 shows the deconvoluted XPS spectra of the GeSn 13% samples with the different contributions of the measured $Ge2p_{3/2}$ orbital, after using those protocols. Upon 40 minutes of air exposure after the H7 treatment (Figure 4b), the fraction of germanium oxide was 45%. This figure decreased down to 21% with the P1 protocol, and 26% with the P2 protocol. Figure 5 shows that the use of a sulfur passivation after the H7 treatment allows to reduce the re-oxidation rate after 40 minutes (21% with sulfur treatment, 45% without). Indeed, $(NH_4)_2S$ treatment allows to passivate chemically germanium dangling bonds in surface and thus prevent oxide bonds. Further surface investigation may be carried out later to better. Therefore, we conclude that ammonium sulfur can be a good solution to protect oxide bonds at the GeSn surface.

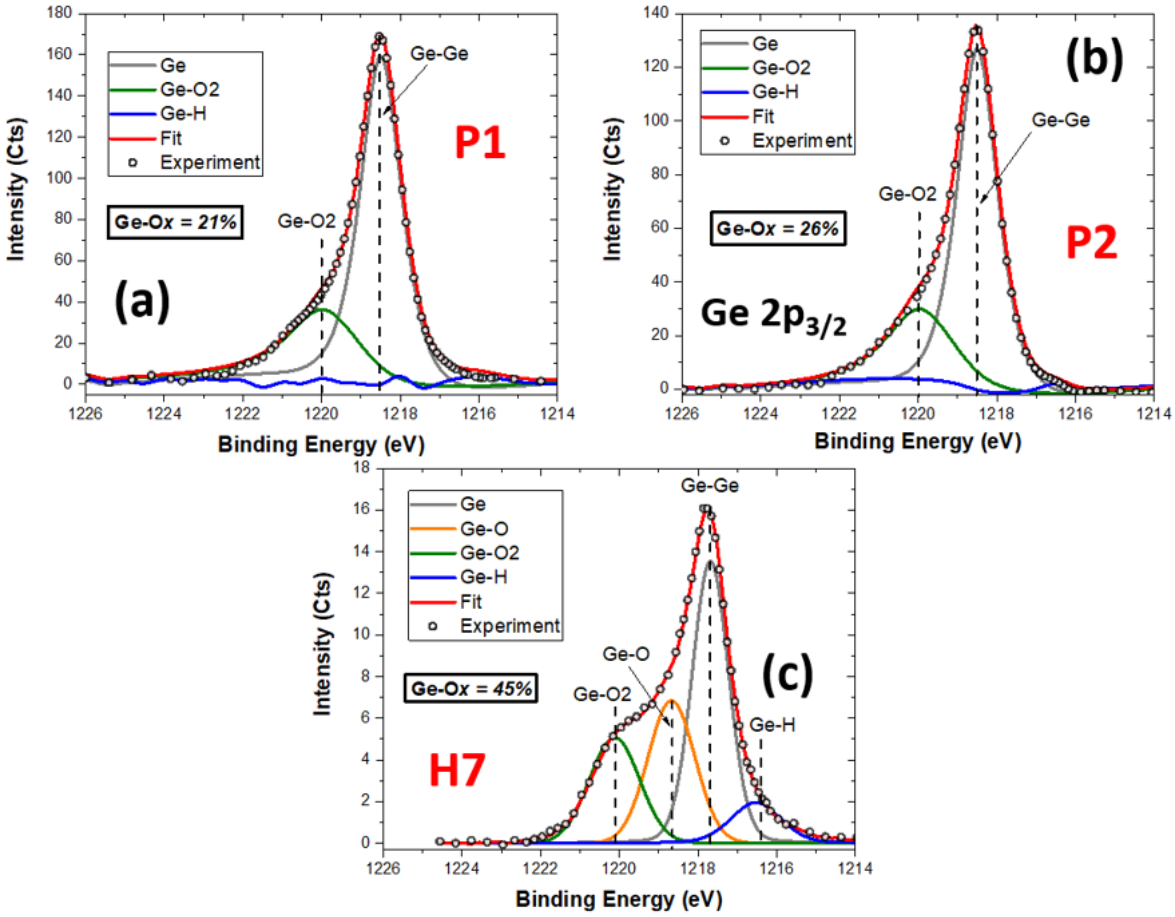

Figure 5: $Ge2p_{3/2}$ XPS spectra after protocols P1 (a), P2 (b), with $(NH_4)_2S$ solutions and H7 (c) showing the partial protection of $Ge_{0.87}Sn_{0.13}$-S bonds to oxidation after 40 min air exposure.

Acronym	Chemical treatment	Amount of Ge oxide
P1	H7 + $(NH_4)_2S$ + DIW	21 %
P2	H7 + DIW + $(NH_4)_2S$ + DIW	26 %
H7	H7 + DIW	45 %

Table 2: Summary of wet treatments used to study the passivation of the GeSn 13% layers.

3.2 Photoemission Electron Momentum Microscopy of the GeSn layer

Band structure measurements on Ge-based epitaxial layers are very challenging [35] because a perfect control of the surface crystallinity and cleanliness is required. For GeSn surfaces, optimal surface preparations prior to *k*PEEM measurements rely on *ex-situ* wet de-oxidation followed by removal of adventitious carbon atoms without any heating or harmful ion etching. Gas Cluster Ion Beams (GCIB, energy = 2eV/atom) in ultra-high vacuum were therefore used, in the XPS chamber, to gently remove unwanted carbon atoms after wet de-oxidation. The low GCIB incident energy ensured that only weakly bonded carbon atoms were removed without any impact on GeSn covalent bonding, preserving thereby the surface crystalline structure. After GCIB, the sample was transferred under an inert atmosphere into the PEEM load-lock chamber which is pumped overnight before kPEEM analysis. After the H7 optimal wet treatment followed by GCIB, it was not possible to observe by *k*PEEM any clear band structure on the GeSn 13% layer. The Sn surface segregation evidenced by XPS depth profiling and Time-Of-Flight Secondary Ion Mass Spectrometry (not shown) most likely hampered a proper band structure analysis. We therefore used a more HCl-concentrated treatment in the form of the H8 recipe (Table 1). With this rough treatment, we were not looking for the most efficient way to remove the GeSn native surface oxide while preserving the surface quality. Here, the H8 treatment was just supposed to remove the surface tin excess and investigate the impact on the obtained kPEEM images. Evidence of a preliminary band structure appeared with this treatment, as shown in Fig. 6 (a) and (b) with *k*PEEM images at -5.22 eV and -0.5 eV below the Fermi level. A significant intensity is observed at the Γ point (center of the field of view) at different binding energies. In the following, we tentatively show the consistency of these data with the band structure of pure Ge (Fig. 6c). In Fig. 6a, the reciprocal distance of 0.89 $\dot{A}^{-1}$ could be associated with the split-off band at -5.22 eV (Figure 6a), a value close to the 1 $\dot{A}^{-1}$ one for pure Ge. Looking now more closely at the image of Fig. 6b, we see that a cut in the first Brillouin zone of GeSn along $K_{//x}$ and $K_{//y}$ is expected to exhibit a 6-fold symmetry, which is what we have here.

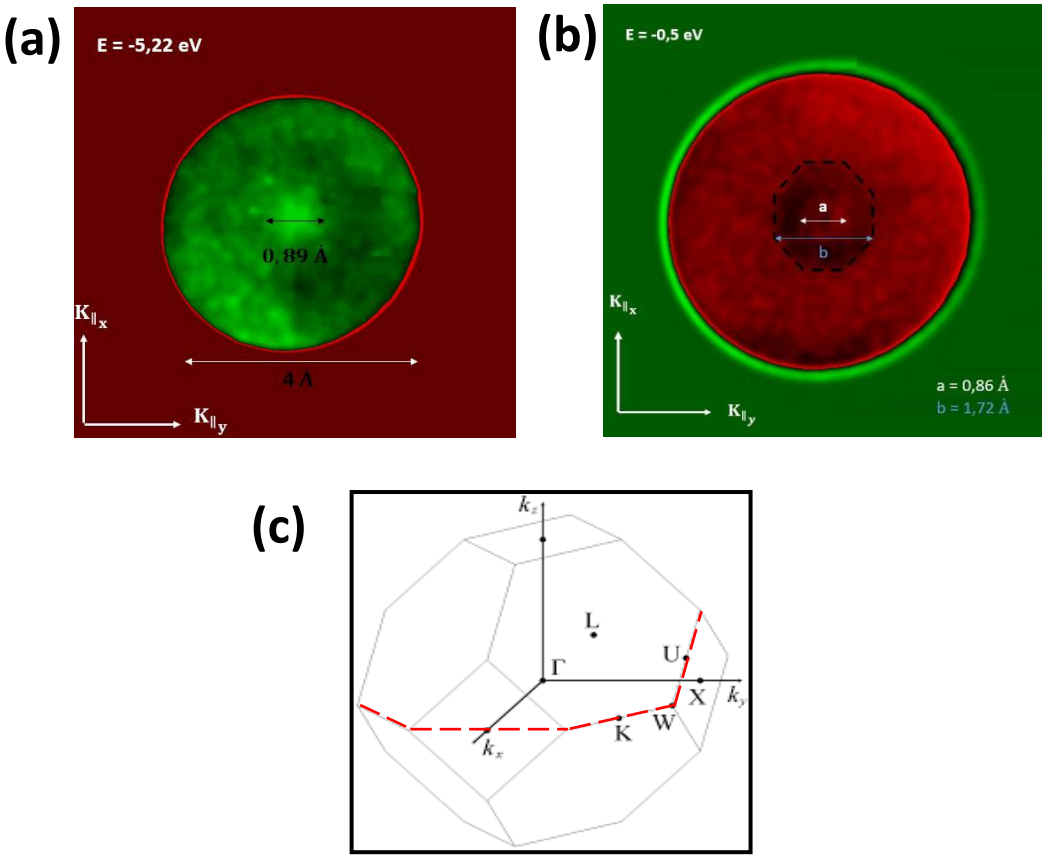

Figure 6: kPEEM images of the GeSn 13% layer: (a) at an energy of -5.22 eV below the Fermi level, (b) at an energy of -0.5 eV below the Fermi level, (c) tentative comparison with the first Brillouin zone of a face-centered cubic Ge lattice [36].

The reciprocal distance separating the Γ and K points (around 0.86 $Å^{-1}$) is a measure of $3\pi/a_{GeSn}$ leading to a distance separating two parallel sides of the octagon of 1.64 $Å^{-1}$, theoretically (Figure 6b). A distance of about 1.72 $Å^{-1}$ is measured on the kPEEM image of Figure 6b. Therefore, the octagon observed at an energy of -0.5 eV would be a section centered at the point Γ of the first Brillouin zone (Figure 6b). For this comparison, we assume that (110) facets dominate the obtained kPEEM images, in agreement with our mention, earlier in the text (AFM section), that <110> surface undulations are the result of plastic strain relaxation. Unfortunately, the weak signal obtained in the kPEEM images, combined also maybe with the limited energy resolution, did not enable us to perform a clear band assignment. More work is necessary towards an optimized ex-situ surface preparation of the GeSn surfaces allowing to extract reliable quantitative informations from cleaner kPEEM images. Therefore the demonstration, at this stage, that kPEEM images are consistent with the Ge band structure is a first step reaching the final aim of preparing ex situ samples for ARPES measurements.

4. Conclusion

The impact of six different HCl/HF-based wet treatments on GeSn 13% surface native oxide removal was evaluated. A 5 min dip in HCl/HF 10%-1% (H7) was found to be the most efficient treatment to remove the GeSn 13% native surface oxide and significantly reduce the surface carbon contamination while maintaining good surface quality. A XPS time-dependent study showed a fast re-oxidation of germanium as opposed to a more stable tin. A $(NH_4)_2S$ post-treatment solution extended the stability of chemically prepared GeSn surfaces exposed to the air, without fully protecting them against native oxide regrowth, however. Band structure measurements by kPEEM on cleaned GeSn surfaces yielded energy bands only after using a relatively aggressive surface treatment. The abnormal behavior of the GeSn surface might be due to an over-concentration of tin close to the GeSn surface (because of Sn segregation in such thick, plastically relaxed layers). After removal of the Sn-rich surface layer, preliminary band structure data were obtained, showing the validity of the overall procedure reported here. However, an optimized route for obtaining ex-situ prepared surfaces allowing reliable ARPES analysis is still needed.

Acknowledgments: This work was supported by the CEA DSM-DRT Phare project "Photonics" the ANR ELEGANTE project and the Gelato Carnot project. Part of this work, carried out on the Platform for Nanocharacterisation (PFNC), was supported by the "Recherche Technologique de Base" program of the French National Research Agency (ANR).

References:

[1] S. Wirths, R. Geiger, N. von den Driesch, G. Mussler, T. Stoica, S. Mantl, Z. Ikonic, M. Luysberg, S. Chiussi, J. M. Hartmann, H. Sigg, J. Faist, D. Buca, D. Grutzmacher, Lasing in direct bandgap GeSn alloy grown on Si (001), Nature Photonics, 9, 88 (2015).

[2] S. Al Kabi, S.A. Ghetmiri, J. Margetis, T. Pham, Y. Zhou, W. Dou, B. Collier, R. Quinde, W. Du, A. Mosleh, J. Liu, G. Sun, R.A. Soref, J. Tolle, B. Li, M. Mortazavi, H.A. Naseem and S.Q. Yu, An optically pumped 2.5 µ m GeSn laser on Si operating at 110 K, Appl. Phys. Lett. 109, 171105 (2016).

[3] V. Reboud, A. Gassenq, N. Pauc, J. Aubin, L. Milord, Q. M. Thai, M. Bertrand, K. Guilloy, D. Rouchon, J. Rothman, T. Zabel, F. Armand Pilon, H. Sigg, A. Chelnokov, J. M. Hartmann, V. Calvo, Optically pumped GeSn micro-disks with 16% Sn lasing at 3.1 µm up to 180 K, Appl. Phys. Lett. 111, 092101 (2017).

[4] Q. M. Thai, N. Pauc, J. Aubin, M. Bertrand, J. Chrétien, V. Delaye, A. Chelnokov, J.-M. Hartmann, V. Reboud, V. Calvo, GeSn heterostructure micro-disk laser operating at 230 K, Opt. Express, 26, 25, 32500–32508 (2018).

[5] J. Chrétien, N. Pauc, F. Armand Pilon, M. Bertrand, Q.-M. Thai, L. Casiez, N. Bernier, H. Dansas, P. Gergaud, E. Delamadeleine, R. Khazaka, H. Sigg, J. Faist, A. Chelnokov, V. Reboud, J.-M. Hartmann, V. Calvo, GeSn Lasers Covering a Wide Wavelength Range Thanks to Uniaxial Tensile Strain, ACS Photonics, 6, 10, 2462-2469 (2019).

[6] Y. Zhou, Y. Miao, S. Ojo, H. Tran, G. Abernathy, J. M. Grant, S. Amoah, G. Salamo, W. Du, J. Liu, J. Margetis, J. Tolle, Y. Zhang, G. Sun, R. A. Soref, B. Li, and S.-Q. Yu, Electrically injected GeSn lasers on Si operating up to 100K, Optica 7, 924–928 (2020).

[7] J. Aubin, J.M Hartmann, A. Gassenq, J.L. Rouviere, E Robin, V. Delaye, D. Cooper, N. Mollard, V. Reboud and V Calvo, Growth and structural properties of step-graded, high Sn content GeSn layers on Ge, Semicond. Sci. Technol. 32, 094006 (2017).

[8] S. Gupta, R. Chen, B. Magyari-Kope, H. Lin, B. Yang, A. Nainani, Y. Nishi, J. S. Harris, K. C. Saraswat, GeSn Technology: Extending the Ge Electronics Roadmap, IEEE 2011 International Electron Devices Meeting,16.6.1−16.6.4 (2011).

[9] S. Gupta, Y.-C. Huang, Y. Kim, E. Sanchez, K. C. Saraswat, Hole Mobility Enhancement Inn Compressively Strained Ge0.93Sn0.07 pMOSFETs, IEEE Electron Device Lett., 34 (7), 831−833 (2013).

[10] S. Wirths, D. Stange, M.-A. Pampillon, A. T. Tiedemann, G. Mussler, A. Fox, U. Breuer, B. Baert, E. San Andres, N. D. Nguyen, J.-M. Hartmann, Z. Ikonic, S. Mantl, D. Buca, High- K Gate Stacks on Low Bandgap Tensile Strained Ge and GeSn Alloys for Field-Effect Transistors. ACS Appl. Mater. Interfaces, 7 (1), 62−67 (2015).

[11] B. Vincent, F. Gencarelli, D. Lin, L. Nyns, O. Richard, H. Bender, B. Douhard, A. Moussa, C. Merckling, L. Witters, W. Vandervorst, R. Loo, M. Caymax, M. Heyns, Biaxial and uniaxial compressive stress implemented in Ge(Sn) pMOSFET channels by advanced reduced pressure chemical vapor deposition developments, ECS Trans., 41, 7, 239–248, (2011).

[12] Y. C. Yeo, G. Han, X. Gong, L. Wang, W. Wang, Y. Yang, P. Guo, B. Liu, S. Su, G. Zhang, C. Xue, B. Cheng, Tin-Incorporated Source/Drain and Channel Materials for Field-Effect Transistors. ECS Trans. 2013, 50 (9), 931−936 (2013).

[13] Y. Yang, G. Han, P. Guo, W. Wang, X. Gong, L. Wang, K. L. Low, Y.-C. Yeo, Germanium−Tin P-Channel Tunneling Field-Effect Transistor: Device Design and Technology Demonstration. IEEE Trans. Electron Devices, 60 (12), 4048−4056 (2013).

[14] S. Wirths, A. T. Tiedemann, Z. Ikonic, P. Harrison, B. Hollander, T. Stoica, G. Mussler, M. Myronov, J. M. Hartmann, D. Grutzmacher, D. Buca, S. Mantl, Band Engineering and Growth of Tensile Strained Ge/(Si)GeSn Heterostructures for Tunnel Field Effect Transistors. Appl. Phys. Lett., 102 (19), 192103 (2013).

[15] S. Gupta, R. Chen, J. S. Harris, K. C. Saraswat, Atomic Layer Deposition of Al_2O_3 on Germanium-Tin (GeSn) and Impact of Wet Chemical Surface Pre-Treatment. Appl. Phys. Lett. 2013, 103 (24), 241601 (2013).

[16] S. Wirths, D. Stange, M.-A. Pampillon, A. T. Tiedemann, G. Mussler,A. Fox,U. Breuer,B. Baert, E. San Andres, N. D. Nguyen, J.-M. Hartmann,Z. Ikonic, S. Mantl, Dan Buca, High- k Gate Stacks on Low Bandgap Tensile Strained Ge and GeSn Alloys for Field-Effect Transistors, ACS Appl. Mater. Interfaces 7, 62−67 (2015).

[17] C. Schulte-Braucks,; K. Narimani,; S. Glass,; N. von den Driesch, ; J. M. Hartmann,; Z. Ikonic,; V. V. Afanasev,; Q. T. Zhao,; S. Mantl, D. Buca, Correlation of Bandgap Reduction with Inversion Response in (Si)GeSn/High-k/Metal Stacks. ACS Appl. Mater. Interfaces, 9 (10), 9102−9109 (2017).

[18] C. Schulte-Braucks,; N. Von Den Driesch, S. Glass,; A. T. Tiedemann,; U. Breuer,; A. Besmehn,; J. M. Hartmann,; Z. Ikonic,; Q. T. Zhao,; S. Mantl,; D. Buca, Low Temperature Deposition of High-k/Metal Gate Stacks on High-Sn Content
(Si)GeSn-Alloys. ACS Appl. Mater. Interfaces, 8 (20), 13133−13139 (2016).

[19] L. Wang, S. Su, W. Wang, X. Gong, Y. Yang, P. Guo, G. Zhang, C. Xue, B. Cheng, G. Han,; Y.-C. Yeo, $(NH_4)_2S$ Passivation for High Mobility Germanium-Tin (GeSn) P-MOSFETs, 2012 International Silicon-Germanium Technology and Device Meeting (ISTDM), 1−2 (2012).

[20] T. Haffner, M. A. Mahjoub, S. Labau, J. Aubin, J. M. Hartmann, G. Ghibaudo, S. David, B. Pelissier, F. Bassani, and B. Salem, Improvement of the electrical performance of $Au/Ti/HfO_2/Ge_{0.9}Sn_{0.1}$ p-MOS capacitors by using interfacial layers, Appl. Phys. Lett. 115, 171601 (2019).

[21] P.E. Raynal, A. Quintero, V. Loupa, Ph. Rodriguez, L. Vallier, J. Aubin, J.M. Hartmanna, N. Chevalier, P. Bessona, GeSn surface preparation by wet cleaning and in-situ plasma treatments prior to metallization, Microelectronic Engineering 203–204, 38–43, (2019).

[22] N. Coudurier, A. Quintero, V. Loup, P. Gergaud, J.-M. Hartmann, D. Mariolle, V. Reboud, P. Rodriguez, Plasma surface treatment of GeSn layers and its subsequent impact on Ni / GeSn solid-state reaction, submitted.

[23] A. Quintero, P. Gergaud, J.-M. Hartmann, V. Delaye, V. Reboud, E. Cassan, P. Rodriguez, Impact and behavior of Sn during the Ni/GeSn solid-state reaction, J. Appl. Cryst., 53, 605-613 (2020).

[24] A. Quintero, P. Gergaud, J.-M. Hartmann, V. Reboud, E. Cassan , P. Rodriguez, Impact of alloying elements (Co, Pt) on nickel stanogermanide formation, Mater. Sci. Semicond. Process., 108, 104890 (2020).

[25] A. Quintero, P. Gergaud, J. Aubin, J.-M. Hartmann, N. Chevalier, J.-. P. Barnes, V. Loup, V. Reboud, F. Nemouchi, P. Rodriguez, Impact of Pt on the phase formation sequence, morphology and electrical properties of Ni(Pt) / Ge0.9Sn0.1 system during solid-state reaction, J. Appl. Phys., 124, 085305 (2018).

[26] M. A. Mahjoub, T. Haffner, S. Labau, E. Eustache, J. Aubin, J.-M. Hartmann, G. Ghibaudo, B. Pelissier, F. Bassani, B. Salem, Impact of Wet Treatments on the Electrical Performance of Ge0.9Sn0.1-Based p-MOS Capacitors, ACS Appl. Electron. Mater. 1, 2, 260–268 (2019).

[27] W. Du, Q. M. Thai, J. Chrétien, M. Bertrand, L. Casiez, Y. Zhou, J. Margetis, N. Pauc, A. Chelnokov, V. Reboud, V. Calvo, J. Tolle, B. Li, Shui-Qing Yu, Study of si-based gesn optically pumped lasers with micro-disk and ridge waveguide structures, Frontiers in Physics, 147 (2019).

[28] M. Bertrand, Q.M. Thai, J. Chrétien , N. Pauc,, R. Khazaka, J. Aubin, O. Lemonnier, A. Chelnokov, J.M. Hartmann, V. Calvo, V. Reboud, Optoelectrical Characterizations of GeSn Heterojunction Photodiodes with 6% to 16% of Sn, IEEE International Conference on Group IV Photonics GFP, 45–46, 8478709 (2018).

[29] M. Bertrand, L. Casiez, A. Quintero, J. Chretien, N. Pauc, Q.M. Thai, R. Khazaka, P. Rodriguez, J.M. Hartmann, A. Chelnokov, V. Calvo, V. Reboud, Vertical GeSn electro-absorption modulators grown on Silicon for the mid-infrared, IEEE Photonics Conference, IPC 2020 - Proceedings, 2020, 9252483 (2020).

[30] J. Aubin and J.M. Hartmann, GeSn growth kinetics in reduced pressure chemical vapor deposition from Ge2H6 and SnCl4, J. Cryst. Growth 482, 30 (2018).

[31] J. Aubin, J.M. Hartmann, A. Gassenq, L. Milord, N. Pauc, V. Reboud and V. Calvo, Impact of thickness on the structural properties of high tin content GeSn layers, J. Cryst. Growth 473, 20 (2017).

[32] M. Escher, N. Weber, M. Merkel, C. Ziethen, P. Bernhard, G. Schönhense, S. Schmidt, F. Forster, F. Reinert, B. Krömker, D. Funnemann, NanoESCA: A novel energy filter for imaging x-ray photoemission spectrosocpy, 17, 16, 27, S1329-S1338 (2005).

[33] M. Escher, K. Winkler, O. Renault, and N. Barrett, Applications of high lateral and energy resolution imaging XPS with a double hemispherical analyser based spectromicroscope, Journal of Electron Spectroscopy and Related Phenomena, 178–179, 303 (2010).

[34] T. Maeda, S. Takagi, T. Ohnishi, M. Lippmaa, Sulfur passivation of Ge (0 0 1) surfaces and its effects on Schottky barrier contact, Mater. Sci. Semicond. Process., 9, 4-5, 706-710, (2006).

[35] T. Sakata, S. Takeda, K. Kitagawa, H. Daimon, Interband interaction between bulk and surface resonance bands of a Pb-adsorbed Ge(001) surface, Semicond. Sci. Technol., 31, 085012 (2016).

[36] Richard M. Martin, Electronic Structure: Basic Theory and Practical Methods, Cambridge University Press (2020).